NUCLEAR THEORY, Vol. 31 (2012)
eds. A. Georgieva, N. Minkov, Heron Press, Sofia

Energies and Transition Probabilities from the Full Solution of Nuclear Quadrupole-Octupole Model

M. Strecker[1], **N. Minkov**[1,2], **H. Lenske**[1]

[1]Institut für Theoretische Physik der Justus-Liebig-Universität, Heinrich-Buff-Ring 16, D–35392 Giessen, Germany

[2]Institute of Nuclear Research and Nuclear Energy, Bulgarian Academy of Sciences, Tzarigrad Road 72, BG-1784 Sofia, Bulgaria

Abstract. A collective model of nuclear quadrupole-octupole vibrations and rotations, originally restricted to a coherent interplay between quadrupole and octupole modes, is now developed for application beyond this restriction. The eigenvalue problem is solved by diagonalizing the unrestricted Hamiltonian in the basis of the analytic solution obtained in the case of the coherent-mode assumption. Within this scheme the yrast alternating-parity band is constructed by the lowest eigenvalues having the appropriate parity at given angular momentum. Additionally we include the calculation of transition probabilities which are fitted with the energies simultaneously. As a result we obtain a unique set of parameters. The obtained model parameters unambiguously determine the shape of the quadrupole-octupole potential. From the resulting wave functions quadrupole deformation expectation values are calculated which are found to be in agreement with experimental values.

1 Introduction

Collective quadrupole and octupole deformations in atomic nuclei, providing vibrational, rotational and transitional structures of the spectra, lead to especially interesting spectra with parity effects in the regions where these deformations coexist. In [1] Minkov *et al.* applied a coherent quadrupole-octupole motion (CQOM) model to several even-even rare-earth nuclei. This model can be solved analytically if one imposes equal frequencies for the quadrupole and octupole motion and the solution is shortly presented below.

The purpose of the present work, in continuation of a previous paper [2], is to include transition probabilities into the model description. This allows for the first time a unique determination of the model parameters which are adjusted so as to reproduce the experimental values in the best way possible. As a consequence, the model potentials and the resulting wave functions are now obtained unambiguously and even allow a prediction of the quadrupole deformation by calculating the β_2 expectation value.

2 Two-dimensional Coherent Quadrupole-Octupole Model

2.1 General Hamiltonian

The starting point is a vibration-rotation Hamiltonian formulated in the collective axial quadrupole and octupole deformation variables β_2 and β_3 [1]

$$H_{qo} = -\frac{\hbar^2}{2B_2}\frac{\partial^2}{\partial\beta_2^2} - \frac{\hbar^2}{2B_3}\frac{\partial^2}{\partial\beta_3^2} + \frac{1}{2}C_2\beta_2^2 + \frac{1}{2}C_3\beta_3^2 + \frac{X(I)}{d_2\beta_2^2 + d_3\beta_3^2}\,, \quad (1)$$

where $X(I) = \frac{1}{2}[d_0 + I(I+1)]$ for even-even nuclei. B_2 and B_3 are mass parameters, C_2 and C_3 are stiffness parameters, d_2 and d_3 are moment of inertia parameters and d_0 determines the potential core at angular momentum $I = 0$.

2.2 Coherent solution

The transition to ellipsoidal coordinates given by

$$\eta = \left[\frac{2(d_2\beta_2^2 + d_3\beta_3^2)}{d_2 + d_3}\right]^{\frac{1}{2}} \quad \text{and} \quad \phi = \arctan\left(\frac{\beta_3}{\beta_2}\sqrt{\frac{d_3}{d_2}}\right) \quad (2)$$

and the imposition of the relations $B := \frac{d}{d_2}B_2 = \frac{d}{d_3}B_3$ and $C := \frac{d}{d_2}C_2 = \frac{d}{d_3}C_3$, where $d = (d_2 + d_3)/2$, allows one to obtain the energy spectrum in the following closed formula [1]

$$E_{n,k} = \hbar\omega\left[2n + 1 + \sqrt{k^2 + b\cdot X(I)}\right]\,, \quad (3)$$

where $\omega = \sqrt{C/B}$ and $b = 2B/\hbar^2 d$ are considered as fitting parameters. The model wave function has the form

$$\Psi^{\pi}_{nIM0}(\eta,\phi) = \sqrt{\frac{2I+1}{8\pi^2}}D^I_{M\,0}(\theta)\Phi^{\pi}_{nkI}(\eta,\phi)\,, \quad (4)$$

where $D^I_{M\,0}(\theta)$ is the Wigner rotation function and

$$\Phi^{\pi}_{nkI}(\eta,\phi) = \psi^I_{nk}(\eta)\varphi^{\pi}_k(\phi) \quad (5)$$

is the quadrupole-octupole vibration function. Here

$$\psi^I_{n,k}(\eta) = \sqrt{\frac{2c\Gamma(n+1)}{\Gamma(n+2s+1)}}e^{-c\eta^2/2}(c\eta^2)^s L_n^{2s}(c\eta^2) \quad (6)$$

is the "radial" part of $\Phi(\eta,\phi)$ with $c = \sqrt{BC}/\hbar$ and $s = (1/2)\sqrt{k^2 + bX(I)}$ as well as

$$\varphi^+_k(\phi) = \sqrt{2/\pi}\cos(k\phi)\,, \quad k = 1,3,5,\ldots \quad (7)$$

$$\varphi_k^-(\phi) = \sqrt{2/\pi}\sin(k\phi)\,, \quad k = 2,4,6,\ldots \tag{8}$$

for the "angular" wave functions with either positive or negative parity.

For the quantum numbers $n = 0,1,2,\ldots$ and $k = 1,2,3,\ldots$ one chooses the lowest possible values to describe the yrast spectra. This means one takes always $n = 0$ and $k = 1$ for even angular momenta (positive parity) and $k = 2$ for odd angular momenta (negative parity). In the case when non-yrast alternating-parity bands are described one needs to consider higher k-values [10].

2.3 Numerical diagonalization

The details about the diagonalization procedure can be found in [2]. The CQOM basis functions $\Phi(\eta,\phi)$ have the advantage to automatically consider the boundary condition of the model, namely that the wave function must vanish along the β_3-axis. An energy cutoff for the number of basis functions is applied and we consider approximately the 30 lowest lying states for the diagonalization. It is checked that this is enough to provide convergence of the results, *i.e.* the results do no longer change if more basis states are added. Furthermore the basis is optimized as explained in [2]. For the integration of the matrix elements we apply a formula which allows one to obtain the numerical values of the definite integrals quickly by means of a generalized hypergeometric function ${}_3F_2$. Then the eigenvalues and eigenvectors of the Hamiltonian matrix are calculated and we construct the model spectrum as described in [2].

2.4 Theory of transition operators

The basic theory about electromagnetic transitions in the coherent case can be found in [1]. Since the consideration is restricted to axial deformations only, the projection K of the collective angular momentum on the principal symmetry axis is taken as zero.

For a given model state $\Psi^{\pi}_{nkIM0}(\eta,\phi)$, a given multipolarity λ as well as initial quantum numbers $n = n_i$, $k = k_i$, $I = I_i$, and final quantum numbers $n = n_f$, $k = k_f$, $I = I_f$, we have

$$\begin{aligned} &B(E\lambda; n_i k_i I_i \to n_f k_f I_f) \\ &= \frac{1}{2I_i+1}\sum_{M_i M_f \mu}\left|\left\langle \Psi^{\pi_f}_{n_f k_f I_f M_f 0}(\eta,\phi)|\mathcal{M}_\mu(E\lambda)|\Psi^{\pi_i}_{n_i k_i I_i M_i 0}(\eta,\phi)\right\rangle\right|^2 . \end{aligned} \tag{9}$$

The operators for the electric E1, E2 and E3 transitions are given by

$$\mathcal{M}_\mu(E\lambda) = \sqrt{\frac{2\lambda+1}{4\pi(4-3\delta_{\lambda,1})}}\hat{Q}_{\lambda 0}D^{\lambda}_{\mu 0}, \quad \lambda = 1,2,3, \quad \mu = 0,\pm1,\ldots,\pm\lambda\,, \tag{10}$$

where

$$\hat{Q}_{10} = M_1\beta_2\beta_3 \qquad \hat{Q}_{\lambda 0} = M_\lambda\beta_\lambda, \qquad \lambda = 2,3\,. \tag{11}$$

For the $\hat{Q}$-operators we use first order expressions in β_2 and β_3 for the E2 and E3 case while for E1 we use the second order expression.

The M_λ factors are electric charge factors which we take as [4]

$$M_\lambda = \frac{3}{\sqrt{(2\lambda+1)\pi}} ZeR_0^\lambda, \qquad \lambda = 2,3\,, \tag{12}$$

where $R_0 = r_0 A^{1/3}$ with $r_0 \approx 1.2$ fm is the nuclear radius, Z is the proton number and e is the electric charge of the proton. The charge factor M_1 is taken according to the droplet model concept [5–7] in the form [9]

$$M_1 = \frac{9AZe^3}{56\sqrt{35}\pi}\left(\frac{1}{J} + \frac{15}{8QA^{\frac{1}{3}}}\right), \tag{13}$$

where the quantities J and Q are related to the volume and surface symmetry energy, respectively. A reasonable choice for them should lie in the regions [8,9]

$$25 \leq J \leq 44 \text{ MeV} \qquad 17 \leq Q \leq 70 \text{ MeV}\,. \tag{14}$$

For practical calculations we choose fixed average values $J = 35$ MeV and $Q = 45$ MeV. We also replace the proton charge e by an effective charge e^1_{eff}, which can have a value different from one and which enters in the fitting procedure as an adjustable parameter.

It was found however that the operators from equation (11) are not sufficient for the CQOM model and have to be modified as follows. In continuation to the above mentioned transition theory, we can write the $\hat{Q}$-operators, Eq. (11), in ellipsoidal coordinates as

$$\hat{Q}_{10} = M_1 pq\eta^2 \cos\phi \sin\phi \tag{15}$$

$$\hat{Q}_{20} = M_2 p\eta \cos\phi \tag{16}$$

$$\hat{Q}_{30} = M_3 q\eta \sin\phi\,. \tag{17}$$

The operators (15)-(17) correspond to a fixed nuclear shape situation with fixed values of β_2 and β_3. In case of the CQOM the density distribution can have many maxima. This phenomenon can be interpreted as a kind of "overtones" related to the coherent collective oscillations of the system. The original operators (15)-(17) cannot take into account multiple maxima in the collective states. As a consequence it was found that using these original operators the B(E3) transition probabilities are vanishing if the difference in the k numbers of the two used wave functions is larger than one.

As explained in [10], this limitation is removed by the introduction of the following replacements:

$$\cos\phi \longrightarrow A_{20}(\phi) \equiv \sum_{k=1}^{\infty} a_{20}^{(k)} \cos(k\phi) \tag{18}$$

$$\sin\phi \longrightarrow A_{30}(\phi) \equiv \sum_{k=1}^{\infty} a_{30}^{(k)} \sin(k\phi)\,. \tag{19}$$

If one choses $a^{(k)} = 1/k$ then the sums are convergent and the limit is known in analytical form.

$$A_{20}(\phi) = \sum_{k=1}^{\infty} \frac{\cos(k\phi)}{k} = -\frac{1}{2}\left[\ln 2 + \ln(1-\cos\phi)\right] \quad (20)$$

$$A_{30}(\phi) = \sum_{k=1}^{\infty} \frac{\sin(k\phi)}{k} = \frac{\pi-\phi}{2} + \pi \text{Floor}\left(\frac{\phi}{2\pi}\right), \quad (21)$$

where the floor function cuts away the digits after the comma and gives the largest previous integer. The angular part of the second order operator can then be generalized by replacing the factors of the product with their generalizations

$$\cos\phi\sin\phi \longrightarrow A_{10}(\phi) \equiv A_{20}(\phi)A_{30}(\phi) = \sum_{m=1}^{\infty}\sum_{n=1}^{\infty} \frac{\cos(m\phi)}{m}\frac{\sin(n\phi)}{n}. \quad (22)$$

If one reduces the sums to only the first summand, the original operators are reobtained. We now redefine the transition operators (15)-(17) as

$$\hat{Q}_{10}(\eta,\phi) = M_1 pq\eta^2 A_{10}(\phi) \quad (23)$$

$$\hat{Q}_{20}(\eta,\phi) = M_2 p\eta A_{20}(\phi) \quad (24)$$

$$\hat{Q}_{30}(\eta,\phi) = M_3 q\eta A_{30}(\phi). \quad (25)$$

If one carries out the integration over the rotational part involving the Wigner D-functions, one is left with

$$B(E\lambda; n_i k_i I_i \to n_f k_f I_f) = \\ = \frac{2\lambda+1}{4\pi(4-3\delta_{\lambda,1})}\langle I_i 0\lambda 0|I_f 0\rangle^2 R_\lambda^2(n_i k_i I_i \to n_f k_f I_f) \quad (26)$$

where the square of a Clebsch-Gordan coefficient appears and R_λ involves integrals of η and ϕ and is given by

$$R_\lambda(n_i k_i I_i \to n_f k_f I_f) = \left\langle \Phi^{\pi_f}_{n_f k_f I_f}(\eta,\phi)|\hat{Q}_{\lambda 0}|\Phi^{\pi_i}_{n_i k_i I_i}(\eta,\phi)\right\rangle. \quad (27)$$

We can advantageously use this coherent theory from [10] to calculate the transition probabilities in the non-coherent case. Since the wave function is expanded with respect to the basis functions and for them the transition theory is known, we obtain for the non-coherent matrix elements the following double sum including known expansion coefficients:

$$\tilde{R}_\lambda(I_i \to I_f) = \sum_{n'k'}\sum_{n''k''} c^{I_f}_{n''k''} c^{I_i}_{n'k'} R_\lambda(n'\,k'\,I_i \to n''\,k''\,I_f). \quad (28)$$

In order to calculate the non-coherent transitions one simply has to replace R_λ with $\tilde{R}_\lambda$ in the above expression (26).

We take into account transition probabilities related to the yrast band. It has been found that this is very important and necessary in order to obtain a set of parameters which is uniquely determined. The reason for this is that one of the fitting parameters, c, only appears in the wave functions. Its value could be arbitrarily chosen in the previous approach without transition probabilities and was chosen in such a way as to approximately reproduce parameter values which lie in a physically reasonable region.

3 Application to Some Nuclei

Once the diagonalizations have been performed for all angular momenta, one obtains an yrast spectrum and is able to define a function σ_{RMS} which gives the root mean square deviation from the experimental levels. The transition probabilities are calculated from the above theory and we construct an overall root mean square deviation function including both energies and transitions. The transitions are included with weight factors providing the same order of magnitude for the fitting procedure.

Then the model parameters B_2, B_3, C_2, C_3, d_2, d_3, d_0 and e^1_{eff} can be adjusted so as to provide the best description of experimental data. As a first guess for the minimization we take the parameter values obtained from the CQOM model.

The model approach was applied to describe the yrast alternating parity spectra and yrast transitions of the nuclei ^{152,154}Sm, ^{154,156}Gd, ^{100}Mo and ^{236}U. The resulting optimal parameters are given in Table 1. It should be kept in mind that the fitting algorithm finds a local minimum and it eventually could be that there is another minimum which provides an even better description. We also calculate the corresponding wave functions for zero angular momentum and the resulting quadrupole deformation expectation values given by

$$\langle\beta_2\rangle = \int_{-\infty}^{\infty}\int_{0}^{\infty} \beta_2 \Phi(\beta_2,\beta_3)^2 d\beta_2 d\beta_3 \,. \tag{29}$$

Table 1. Parameters of the fits obtained for ^{152,154}Sm, ^{154,156}Gd, ^{100}Mo and ^{236}U. The parameters B_2, B_3 are given in units of $\hbar^2$/MeV, C_2 and C_3 are given in units of MeV, d_2 and d_3 are given in $\hbar^2\cdot\text{MeV}^{-1}$, d_0 is given in $\hbar^2$ and e^1_{eff} is in units of elementary charge.

Nucleus	B_2	B_3	C_2	C_3	d_2	d_3	d_0	e^1_{eff}
^{152}Sm	26.0	334.9	68.8	368.5	836.9	3886.7	24.3	1.43
^{154}Sm	2.9	339.0	111.2	2443.0	330.4	12264.9	325.8	1.64
^{154}Gd	7.5	172.5	85.8	482.7	486.7	4190.8	70.8	1.88
^{156}Gd	6.2	337.9	193.3	1257.6	954.7	7395.0	153.9	0.95
^{100}Mo	0.437	16.9	11379.9	87.6	682.2	577.5	18.9	0.56
^{236}U	186.7	185.6	44.9	619.5	549.8	11475.9	258.2	0.27

The wave functions are plotted in Figures 1-6 and the obtained quadrupole deformations are given in Table 2.

Table 2. Quadrupole deformations obtained from the wave functions for ^{152,154}Sm, ^{154,156}Gd, ^{100}Mo and ^{236}U. The experimental values are taken from RIPL-2 [3].

Nucleus	β_2^{exp}	β_2^{theo}	Nucleus	β_2^{exp}	β_2^{theo}	Nucleus	β_2^{exp}	β_2^{theo}
^{152}Sm	0.3064	0.191	^{154}Gd	0.3120	0.250	^{100}Mo	0.2309	0.135
^{154}Sm	0.3410	0.318	^{156}Gd	0.3378	0.217	^{236}U	0.2821	0.272

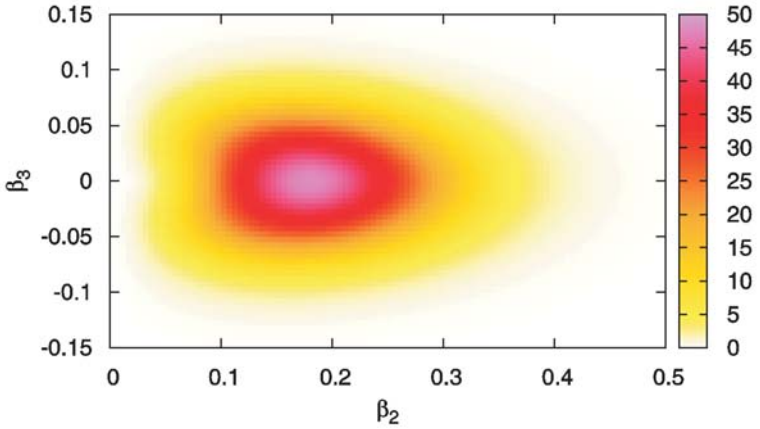

Figure 1. Wave function for ^{152}Sm at angular momentum $I = 0$.

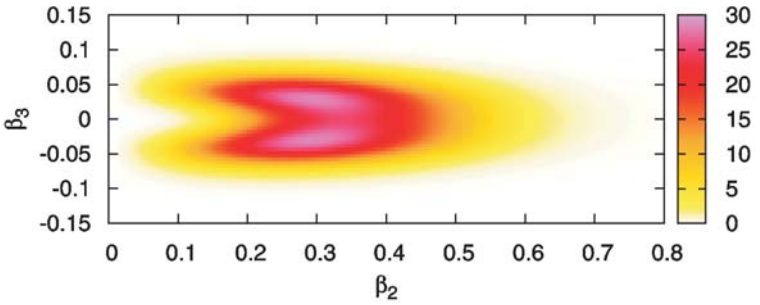

Figure 2. Wave function for ^{154}Sm at angular momentum $I = 0$.

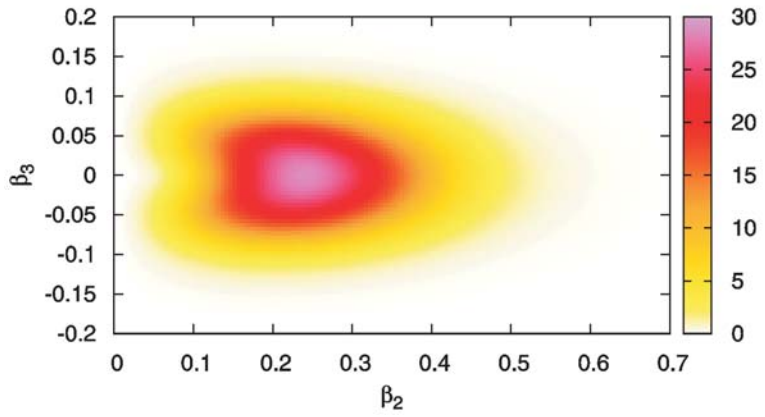

Figure 3. Wave function for ^{154}Gd at angular momentum $I = 0$.

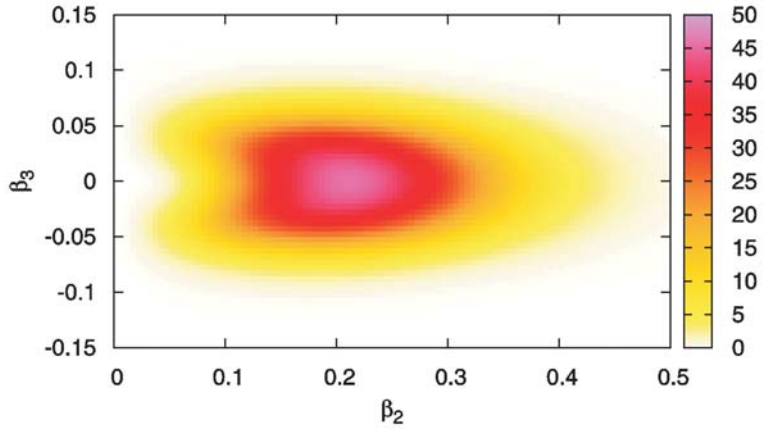

Figure 4. Wave function for ^{156}Gd at angular momentum $I = 0$.

4 Discussion and Outlook

As already shown in [2] the numerical solution of the CQOM model leads to a better description of the yrast spectra. We expect that in this previous approach where only energies were used for the fitting procedure one obtains a better root mean square (RMS) value for the energies than in the present work. This is due to the fact that here we also simultaneously fit transition probabilities in addition to the energies. For two nuclei this is checked in Table 3. While we see our expectation confirmed in the case of ^{152}Sm, we surprisingly notice that in case of ^{154}Gd the RMS value for the energies is even better than the value of

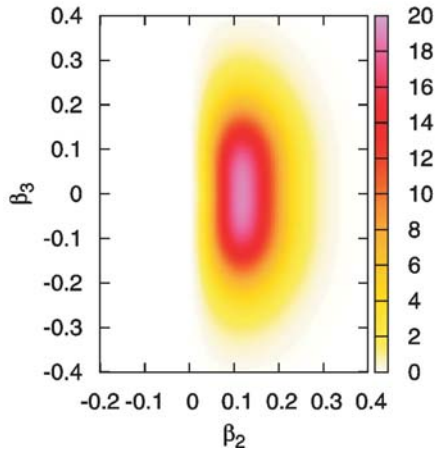

Figure 5. Wave function for ^{100}Mo at angular momentum $I = 0$.

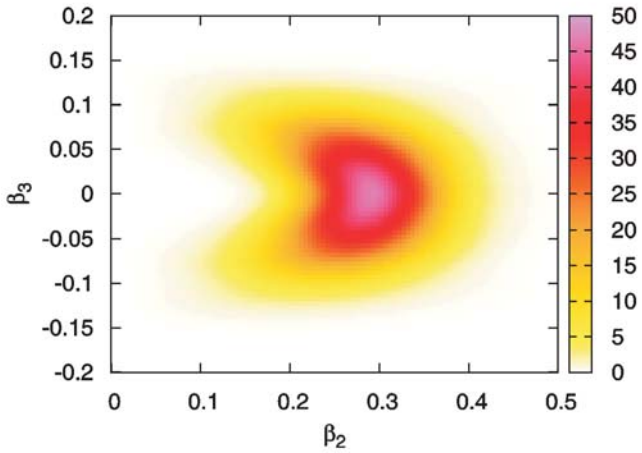

Figure 6. Wave function for ^{236}U at angular momentum $I = 0$.

Table 3. Root mean square deviations for the energies for two nuclei which were considered in the CQOM model [10] (left column), in the previous paper [2] about energy levels only in the non-coherent case (middle column) as well as in the present approach (right column).

Nucleus	σ_{CQOM} [keV]	σ_{en} [keV]	$\sigma_{\text{en+trans}}$ [keV]
^{152}Sm	48.7	23.3	47.5
^{154}Gd	74.0	47.0	44.8

Table 4. Theoretical and experimental values of B(E1), B(E2) and B(E3) transition probabilities in Weisskopf units (W.u.) for the alternating-parity spectrum of ^{152}Sm. Notations: g (ground-state band) and n1 (first negative-parity band). The data is taken from [11] except for the E3-transition, which is taken from [12]. Only transitions involving the yrast band are considered. The uncertainties (in parentheses) refer to the last significant digits in the experimental data.

Mult	Transition	Exp [W.u.]	Theo [W.u.]	Weight
E2	$2_g \rightarrow 0_g$	144(3)	142	10
E2	$4_g \rightarrow 2_g$	209(3)	212	10
E2	$6_g \rightarrow 4_g$	245(5)	250	10
E2	$8_g \rightarrow 6_g$	285(14)	284	10
E2	$10_g \rightarrow 8_g$	320(3)	318	10
E1	$1_{n1} \rightarrow 0_g$	0.0042(4)	0.0042	100000
E1	$1_{n1} \rightarrow 2_g$	0.0077(7)	0.0088	100000
E1	$3_{n1} \rightarrow 2_g$	0.0081(16)	0.0057	100000
E1	$3_{n1} \rightarrow 4_g$	0.0082(16)	0.0083	100000
E3	$3_{n1} \rightarrow 0_g$	14(2)	20	10

the previous approach. This is an indication that the parameters of the previous approach are not optimal and a better parameter set is found in the present work.

In order to get an idea about the quality of the fitted transitions Table 4 provides some data from the experiment as well as theoretical values. As one can see, the agreement is quite good and most often in agreement with the error bars.

One main result is that with the inclusion of transition probabilities into the fitting procedure we obtain unique parameters which additionally lie in a physically reasonable region.

Another impressive result which can be seen from Table 2 is that – without fitting these quantities – the quadrupole deformation expectation values are obtained reasonably and they reproduce the behaviour given by the experiment for the different nuclei, especially the least deformed nucleus in the experiment is also least deformed in the theory and the same holds for the most deformed nucleus. The octupole deformation (not shown here) can be obtained in a similar way by localizing the maximum of the wave function in the quadrant with both positive β_2 and β_3 for angular momentum $I = 1$.

Also the shapes from the wave functions seem to change according to the region of nuclei. We observe that the wave functions for the rare-earth nuclei ^{152,154}Sm and ^{154,156}Gd look quite similar while the one for ^{100}Mo looks very different. The shape of the wave function for ^{236}U is similar to the rare-earth case but still different since it looks more heart-shaped.

Concerning future improvements, one could look not only for yrast states but also for higher lying states for which experimental data also exists. However, first test calculations have shown that the overall description of the levels in terms of the RMS deviation becomes much worse in this case. This is due to

the fact that we do not have good quantum numbers n and k in the non-coherent case and therefore cannot reproduce the "jumping" over quantum numbers as it is done in the analytic coherent case [10].

Secondly, one could extend the formalism also to odd-A nuclei. Preliminary work in this direction has already been done.

Acknowledgements

This work is supported by DFG and HIC for FAIR.

References

[1] N. Minkov, P. Yotov, S. Drenska, W. Scheid, D. Bonatsos, D. Lenis and D. Petrellis, *Phys. Rev. C* **73** (2006) 044315.

[2] M. Strecker, N. Minkov and H. Lenske, Full solution of nuclear quadrupole-octupole model, *Nuclear Theory* **30**, Proceedings of the 30th International Workshop on Nuclear Theory (Rila, Bulgaria 2011), ed. A.I. Georgieva and N. Minkov, (Heron Press, Sofia, 2011), p. 53.

[3] Reference Input Parameter Library, www-nds.iaea.org/ripl2/.

[4] G.A. Leander, Y.S. Chen, *Phys. Rev. C* **37** (1988) 2744.

[5] W.D. Myers and W.J. Swiatecki, *Ann. Phys*. **84** (1974) 186.

[6] W.D. Myers: Droplet model of atomic nuclei (IFI/Plenum Data, New York, 1977).

[7] C.O. Dorso, W.D. Myers and W.J. Swiatecki, *Nucl. Phys. A* **451** (1986) 189.

[8] V.Yu. Denisov and A.Ya. Dzyublik, *Nucl. Phys. A* **589** (1995) 17.

[9] P.A. Butler and W. Nazarewicz, *Nucl. Phys. A* **533** (1991) 249.

[10] N. Minkov, S. Drenska, M. Strecker, W. Scheid and H. Lenske, *Phys. Rev. C* **85** (2012) 034306.

[11] http://www.nndc.bnl.gov/nudat2/indx adopted.jsp.

[12] T. Kibedi and R.H. Spear, *At. Data Nucl. Data Tables* **80** (2002) 35-82.